



Electronic structures and thermodynamic properties of HfAl₃ in L1₂, D0₂₂ and D0₂₃ structures

Run-yue LI¹, Yong-hua DUAN^{1,2}

1. School of Materials Science and Engineering, Kunming University of Science and Technology, Kunming 650093, China;

2. Key Lab of Advance Materials in Rare & Precious and Nonferrous Metals, Ministry of Education, Kunming University of Science and Technology, Kunming 650093, China

Received 26 October 2015; accepted 8 April 2016

Abstract: To better understand the relative stability and bonding characteristics of the L1₂, D0₂₂ and D0₂₃ structures for HfAl₃, the formation enthalpies, electronic structures and thermodynamics properties were investigated by first-principles calculations. The agreement of calculated equilibrium lattice parameters and formation enthalpies with experimental results indicates the reliability of this work. The order of structural stability is D0₂₃>D0₂₂>L1₂. The results of densities of states, atomic Mulliken charge and bond population support the best structural stability for D0₂₃ structure. Variations of thermodynamic properties with temperature were predicted via phonon frequencies calculation. The enthalpy, entropy, free energy of D0₂₃ structure change more quickly than those of the other two structures. The Debye temperatures of L1₂, D0₂₂ and D0₂₃ structures are 399, 407 and 416 K, respectively. The volume thermal expansions for HfAl₃ increase exponentially at the low temperature, whereas the thermal expansion coefficients increase linearly at the high temperature.

Key words: first principles calculations; HfAl₃; electronic structure; thermodynamics properties

1 Introduction

The early-transition-metal trialuminides TMAI₃ (TM=Sc, Ti, Zr, Hf, etc) have been attracted great interest due to their low densities, high melting points and low oxidation resistances. These trialuminides are being investigated to be used as single phase high-temperature structural materials and as precipitation strengtheners in two-phase aluminum alloys [1]. In these trialuminides, TiAl₃, VAl₃, NbAl₃ and TaAl₃ crystallize in the tetragonal D0₂₂ structure, while ZrAl₃ embodies in the tetragonal D0₂₃ structure [2,3]. ScAl₃ and YAl₃ are found to be the cubic L1₂ structure at high temperature [2,3]. As an important adding element to increase the recrystallization resistance and structural stability of aluminum alloys, Hf makes the extruded aluminum alloys meet the demand of tolerant of high temperature by forming HfAl₃ dispersoids [4]. HfAl₃ crystallizes in the D0₂₃ structure at low temperature, the D0₂₂ structure at high temperature [5] and the metastable

L1₂ structure [1].

Due to the lack of sufficient number of slip systems for the D0₂₂ structure, the L1₂ structure has been proved experimentally that it is more ductile than the D0₂₂ structure [6]. Accordingly, the L1₂-trialuminide alloys are more likely to be suitable in structural applications [7]. By rapid solidification of supersaturated Al-rich solid solutions [8–11], chill casting and gas atomization [12,13], and mechanical alloying [1,14], the metastable L1₂-HfAl₃ had been prepared. However, the L1₂-HfAl₃ may transform to D0₂₂ or D0₂₃ structures during the heating process: a transformation of L1₂ to D0₂₃ at 750 °C had been observed [1].

Few theoretical and experimental works have been reported on HfAl₃ compounds. Only their structural properties, phase stability and bulk moduli have been considered. The D0₂₂ unit cell consists of two L1₂ cubes stacked along *z* direction with *a* [1/2 1/2 0] antiphase shift between the cubes, while the D0₂₃ structure consists of a stacking of four L1₂ cubes with the same antiphase shift every two cubes [15]. The order of relative

stabilities of L1₂, D0₂₂, and D0₂₃ structures in the HfAl₃ compounds from their formation enthalpies is D0₂₃>D0₂₂>L1₂ [15]. The reported isothermal bulk modules of these HfAl₃ compounds indicate that the value for each structure is very close to each other [15,16]. To our best knowledge, theoretical investigations on electronic structures and thermodynamic properties of HfAl₃ are still scarce. The reason of difference in stability for these HfAl₃ is still not clear. Additionally, in ordered intermetallics, physical and mechanical properties depend strongly on the nature of the bonding between atomic species.

In this work, to better understand the relative stability, bonding characteristics and thermodynamic properties of the L1₂, D0₂₂ and D0₂₃ structures HfAl₃, we performed calculations of the formation enthalpy, electronic structures and phonon dispersions of HfAl₃ in three different crystal structures using the density-functional theory (DFT) as implemented in the first-principles calculations with the generalized gradient approximation (GGA). Such structural stability and electronic structure studies can provide guidance in other TM trialuminides as well.

2 Methods and computational details

2.1 First-principles method

In the present work, the first principles calculations based on density functional theory (DFT) implemented in Cambridge sequential total energy package (CASTEP) code [17] were carried out to investigate the formation enthalpies and electronic structures. Ultra soft pseudo-potential (USPP) was employed to indicate the interactions between ionic core and valence electrons. The generalized gradient approximation (GGA) with the Perdew-Burke-Ernzerhof (PBE) parameterization [18] was used to describe the exchange correlation energy. Valence electrons included in this work for distinct atoms were Al 3s²3p¹ and Hf 5s²5p⁶5d²6s². After convergence tests, the *k*-points were 20×20×20, 20×20×12 and 20×20×6 for L1₂-HfAl₃, D0₂₂-HfAl₃ and D0₂₃-HfAl₃, respectively, and the cutoff energy for plane wave expansions was set as 500 eV.

The phonon calculations were performed by using the linear response method applied Norm-conserving pseudo-potential. The *k*-point meshes of 12×12×12, 12×12×8 and 12×12×4 were applied along with the cutoff energy of 500 eV for L1₂, D0₂₂ and D0₂₃ structures, respectively. The thermodynamic properties of HfAl₃ were obtained via the resultant phonon dispersion.

2.2 Thermodynamics properties

Based on the phonon calculations, the enthalpy (*H*),

free energy (*F*), heat capacity (*C_V*) and entropy (*S*) as functions of temperature at the finite temperature can be computed. The vibrational contributions to the thermodynamic parameters were evaluated by the Debye's quasi-harmonic approximation (QHA) [19,20]:

$$H(T) = E_{\text{tot}} + E_{\text{zp}} + \int \frac{h\omega}{\exp[h\omega/(kT)] - 1} F(\omega) d(\omega) \quad (1)$$

$$F(T) = E_{\text{tot}} + E_{\text{zp}} + kT \int \ln\{1 - \exp[-h\omega/(kT)]\} F(\omega) d(\omega) \quad (2)$$

$$C_V(T) = k \int \frac{[h\omega/(kT)]^2 \exp[h\omega/(kT)]}{\exp[h\omega/(kT)] - 1} F(\omega) d(\omega) \quad (3)$$

$$S(T) = k \int \frac{h\omega/(kT)}{\exp[h\omega/(kT)] - 1} F(\omega) d(\omega) - k \int \{1 - \exp[-h\omega/(kT)]\} F(\omega) d(\omega) \quad (4)$$

where *E_{tot}* is the total energy of the system, *E_{zp}* is the zero point vibrational energy, *ω* is the phonon vibration frequency, *F(ω)* is phonon density of state, *k* and *h* are Boltzmann's constant and Planck's constant, respectively.

The Debye temperatures *Θ_D* can be estimated from the heat capacity *C_V* by the following equations [21]:

$$C_V(T) = 9nk \left(\frac{T}{\Theta_D} \right)^3 \int_0^{\frac{\Theta_D}{T}} \frac{x^4 \exp x}{(\exp x - 1)^2} dx \quad (5)$$

$$x = \frac{h\omega}{kT} \quad (6)$$

where *n* is the number of atoms in the molecule.

From the obtained phonon dispersion, the thermal expansion coefficients for HfAl₃ are calculated by the Debye-Grüneisen model [22]:

$$\beta = \frac{\gamma C_V}{BV} \quad (7)$$

$$\gamma = -\frac{d(\ln \Theta(V))}{d(\ln V)} \quad (8)$$

where *β* is the volume thermal expansion coefficient; *γ*, *C_V*, *B* and *V* are Grüneisen parameter, heat capacity, bulk modulus and volume, respectively; *Θ(V)* is the Debye temperature. The bulk modules of these HfAl₃ compounds used in the Eq. (7) are quoted from the reported values [16].

3 Results and discussion

3.1 Structural stability

The initial crystal structures of HfAl₃ in L1₂, D0₂₂ and D0₂₃ structures are illustrated in Fig. 1. The calculated structural parameters, together with the

experimental values [23–25], are listed in Table 1. It is found from Table 1 that the calculated lattice parameters agree very well with the available experimental data, whose average deviation is less than 1%. This provides a confirmation that the present utilized computational methodology is suitable and reliable.

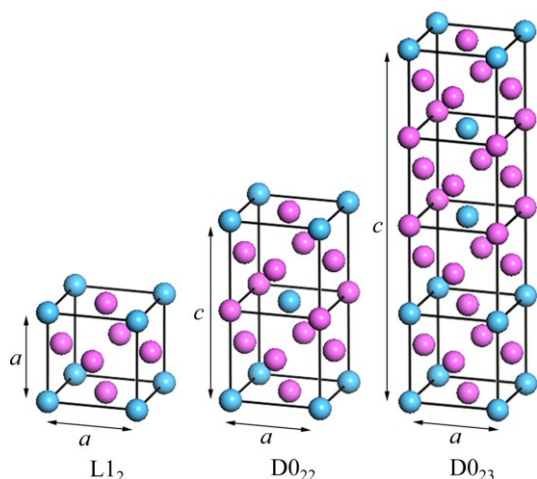


Fig. 1 Initial crystal structures for HfAl₃ in L1₂, D0₂₂ and D0₂₃ structures (Purple and cyan balls demote Al and Hf atoms, respectively)

To investigate the structural stability, the formation enthalpy (ΔH) was calculated by the following expression:

$$\Delta H = \frac{1}{4} [E_{\text{total}} - (E_{\text{Hf}}^{\text{bulk}} + 3E_{\text{Al}}^{\text{bulk}})] \quad (9)$$

where E_{total} is the total energy of HfAl₃, $E_{\text{Hf}}^{\text{bulk}}$ and $E_{\text{Al}}^{\text{bulk}}$ are the total energy of a Hf atom and an Al atom in the bulk state. A more negative formation enthalpy corresponds to a better structural stability. The calculated formation enthalpies of the HfAl₃ compounds, together with the available experimental and other theoretical data [16,26], are also listed in Table 1. From Table 1, the formation enthalpies in our work are in good agreement with the ab initio approach and experiment, and the difference in formation enthalpy between our results and reported values is less than 1 kJ/mol. The order of formation enthalpy is D0₂₃<D0₂₂<L1₂. This suggests that the order of structural stabilities of L1₂, D0₂₂, and D0₂₃ structure is D0₂₃>D0₂₂>L1₂, which is in good agreement

with the report in Ref. [15]. Actually, D0₂₃-HfAl₃ is a stable phase at the temperature below 650 °C, while D0₂₂-HfAl₃ is a stable phase at the temperature higher than 650 °C [27]. When metastable L1₂-HfAl₃, which is detected in Al–Hf bilayers, is heated, it transforms either in D0₂₂ or D0₂₃ structures depending on the temperature [23]. It must be noted that, in the experiment, the transformation of L1₂ to D0₂₃ at 750 °C was observed, but the transformation of D0₂₃ to D0₂₂ by heating at higher temperatures was not found [1].

3.2 Electronic structures

The densities of states, including total and partial densities of states (TDOS and PDOS), in terms of the chemical bonding in HfAl₃ compounds were investigated to understand the structural stability. The results of densities of states are plotted in Fig. 2. One can see that the total densities of states for all structures have a similar shape characterized by the presence of pseudogap near the Fermi level (E_{F}) for HfAl₃ compounds. The right part of the TDOS corresponds to nonbonding states, while the left part refers to bonding states. In the L1₂ structure, E_{F} lies on the right of the minimum of TDOS, whereas in D0₂₂ structure the E_{F} locates on the left of the maximum of the TDOS. The E_{F} of D0₂₃ structure exactly situates at the pseudogap. The TDOS values at the E_{F} for L1₂, D0₂₂ and D0₂₃ structures are 1.74, 1.33 and 1.13 electron/eV per unit cell, respectively. It is interesting to compare the TDOS and formation enthalpies of L1₂, D0₂₂ and D0₂₃ structures that the most negative formation enthalpy corresponds to the lowest TDOS value at the E_{F} . This suggests that D0₂₃ structure with the low TDOS value can more easily reaches the maximum band-filling state than D0₂₂ and L1₂ structures, resulting in the most stable compound for D0₂₃-HfAl₃.

It can be seen in the PDOS that the left part of the TDOS ranging from –6 to 0 eV for HfAl₃ compounds are contributed by a strong hybridization between Hf 5d states and Al 3p states. As a result, the strong Hf–Al atomic bonds form. The Hf d-DOSs at the E_{F} for L1₂, D0₂₂ and D0₂₃ structures are 0.73, 0.73 and 0.56 electron/eV formula unit, respectively. The Al p-DOSs at the E_{F} for L1₂, D0₂₂ and D0₂₃ structures are 0.63, 0.48 and 0.41 electron/eV per unit cell, respectively. The decreasing DOS will result in an increase in the degree

Table 1 Calculated and experimental lattice parameters and formation enthalpies for HfAl₃ compounds

Compound	Present		Experiment		$\Delta H/(\text{kJ} \cdot \text{mol}^{-1})$		
	$a/\text{\AA}$	$c/\text{\AA}$	$a/\text{\AA}$	$c/\text{\AA}$	Present	ab initio [16]	Experiment [26]
L1 ₂ -HfAl ₃	4.096		4.080 [23]		–36.454	–36.828	
D0 ₂₂ -HfAl ₃	3.946	8.924	3.928 [24]	8.888	–38.991	–38.649	
D0 ₂₃ -HfAl ₃	4.002	17.226	3.989 [25]	17.155	–39.224	–39.632	–40.6±0.8

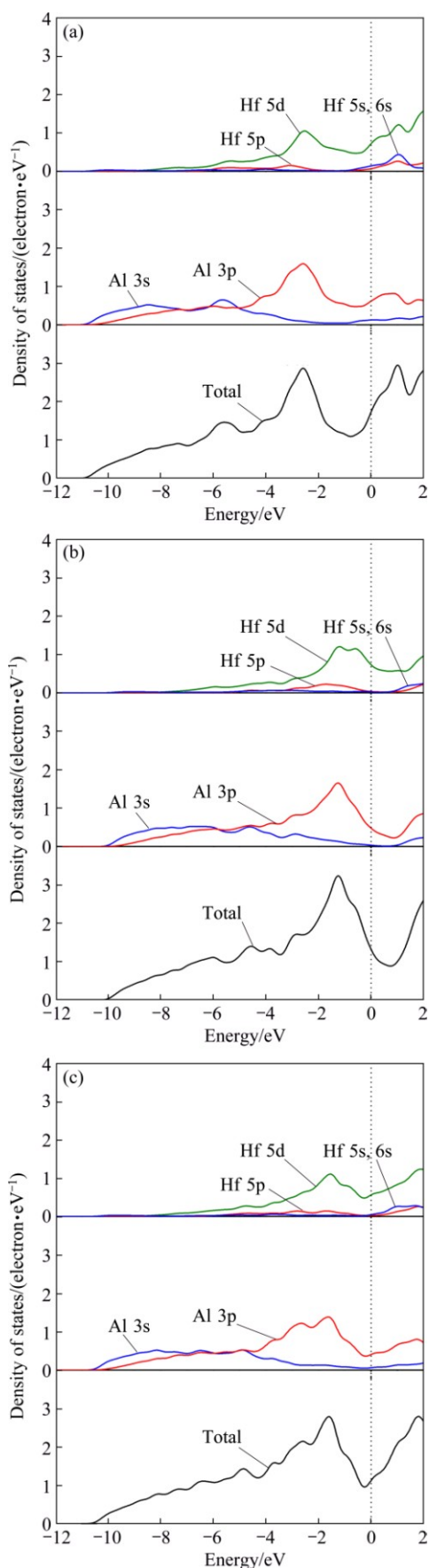


Fig. 2 Calculated TDOS and PDOS of $L1_2$ (a), $D0_{22}$ (b) and $D0_{23}$ (c) structures (The vertical lines indicate the Fermi level)

of hybridization as it has already seen in TiM (M=Fe, Co, Ni) compounds [28]. Thus, the degree of hybridization of the d–p states between Hf and Al atoms increases. In other words, the strength of the d–p bond increases from $L1_2$, $D0_{22}$ to $D0_{23}$ structures. Therefore, the stability of the compounds decreases in the order of $L1_2 < D0_{22} < D0_{23}$ because of the degeneracy of the d–p states at the E_F .

Table 2 lists the atomic Mulliken charge and bond population results of $L1_2$, $D0_{22}$ and $D0_{23}$ HfAl₃ compounds. It is clear that Hf atoms loss electrons and Al atoms get electrons. The number of electrons transferred from Hf to Al in $D0_{23}$ structure is 0.68 (0.17×4), which is larger than those in $L1_2$ ($0.21 \times 1 = 0.21$) and $D0_{22}$ ($0.12 \times 2 = 0.24$) structures. This indicates that the Hf–Al bonds in $D0_{23}$ structure are stronger than those in $L1_2$ and $D0_{22}$ structures. From Table 2, the calculated bond populations are positive, suggesting that the Hf–Al bonds are characterized as covalent. The greater Hf–Al bond population and shorter Hf–Al bond length in $D0_{23}$ structure mean that covalent features are stronger in $D0_{23}$ structure than those in $L1_2$ and $D0_{22}$ structures.

The metallicity of the HfAl₃ compound can be calculated by Ref. [29].

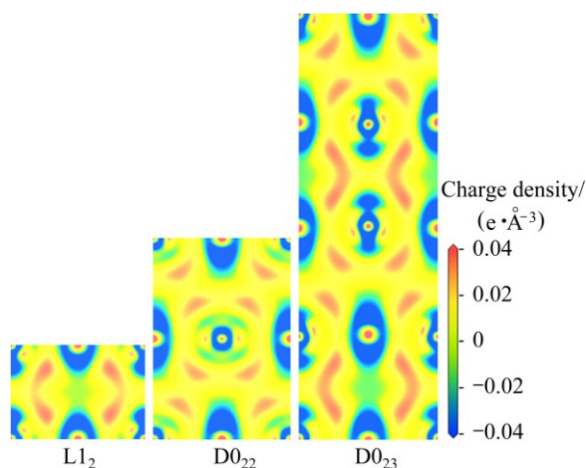
$$f_m = 0.026 D_f / n_e \quad (10)$$

where D_f is the DOS value at E_F , n_e is the valence electronic density of the cell and can be obtained from $n_e = N / V_{\text{cell}}$ (N is the total number of valence electrons and V_{cell} is the cell volume). The calculated values of f_m for $L1_2$, $D0_{22}$ and $D0_{23}$ structures are 0.2393, 0.1645 and 0.0911, respectively. This means that the metallic feature of bonding is in a decreasing order from $L1_2$ to $D0_{23}$ structures.

To further reveal the covalent feature, the charge density difference, which can directly reflect the bonding characteristics [30], was investigated in this work. The results are plotted in Fig. 3. The contours are plotted from $-0.04 \text{ e}/\text{\AA}^3$ to $0.04 \text{ e}/\text{\AA}^3$ with $0.02 \text{ e}/\text{\AA}^3$ interval. From Fig. 3, the extremely localized nature of electronic charge between Hf and Al atoms in these HfAl₃ shows their strong covalent characters. Due to the individualized nature of charge among Al atoms, as a result, the bonding between Al and Al is metallic. Obviously in Fig. 3, the charge density of Al site is more negative than that of Hf site, indicating that there is electron transfer from Hf atom to Al atom. The number of electrons transferred has been discussed in the Mulliken population analysis. The bonding charges in $L1_2$ mainly locate at the tetrahedral interstices along the [111] direction, whereas in $D0_{23}$ it locates along the [112] direction. This is because of the Hf-d hybridization around its local field leading by the nearest-neighbor

Table 2 Atomic Mulliken charge and bond population analysis of HfAl₃ compounds

Structure	Atom	Charge number				Electron number	Bond	Population	Length/Å
		s	p	d	Total				
L1 ₂	Hf1:1a	0.31	0.15	3.33	3.79	0.21	Al _{3c} —Hf (3)	0.24	2.896
	Al3:3c	1.08	1.99	0	3.07	-0.07			
D0 ₂₂	Hf1:2a	0.33	0.28	3.27	3.88	0.12	Al _{2b} —Hf (2)	1.43	2.790
	Al1:2b	1.12	1.77	0	2.89	0.11	Al _{4d} —Hf (8)	0.04	2.978
	Al2:4d	1.08	2.04	0	3.12	-0.12			
D0 ₂₃	Hf1:4e	0.29	0.22	3.32	3.83	0.17	Al _{4c} —Hf (8)	0.10	2.873
	Al1:4c	1.07	2.04	0	3.11	-0.11	Al _{4d} —Hf (8)	0.08	2.945
	Al2:4d	1.08	2.01	0	3.09	-0.09	Al _{4e} —Hf (4)	1.36	2.831
	Al3:4e	1.10	1.87	0	2.97	0.03			

**Fig. 3** Contour plots for electronic charge densities of (110) plane containing Hf and Al atoms (The Hf and Al sites in the charge density maps correspond to those in the crystal structures)

atoms of Hf site. For D0₂₂ structure, the bonding charges primarily locate along the [111] direction caused by the Al-p and Hf-d hybridization. The clear directionality of the bonding also suggests its covalent character in these HfAl₃ compounds.

3.3 Phonon and thermodynamic properties

The phonon dispersion curve, which is related to the lattice dynamical properties of solids, determines the specific heat capacity, heat transportation and sound velocity. Figure 4 plots the calculated phonon dispersions and phonon densities of states (PHDOS) for HfAl₃ compounds. Obviously, no soft modes can be observed at any high-symmetry direction in the phonon dispersion curves. This confirms the stability of the L1₂, D0₂₂ and D0₂₃ structures. The phonon dispersions of L1₂, D0₂₂ and D0₂₃ structures are significantly different because of their different symmetry. The unit cells of L1₂, D0₂₂ and D0₂₃ structures have 4, 8 and 16 atoms, respectively. This suggests that the total numbers of phonon branches are

12, 24 and 48 for L1₂, D0₂₂ and D0₂₃ structures, respectively. The shapes of the phonon dispersion curves and PHDOS are determined by the atomic mass of Hf and Al. It is obvious that the shapes of phonon dispersion and PHDOS of L1₂ structure exhibit large difference from those of D0₂₂ and D0₂₃ structures. This shows that the large atomic mass difference between Hf and Al results in the obvious divergences in the phonon dispersion and PHDOS of L1₂ structure. The acoustic branches in the low frequency region are contributed from the Hf atom, while the optical branches come from the Al atom. The frequencies increase from L1₂, D0₂₂ to D0₂₃ structures due to the difference in lattice constants and bond lengths. It has been shown in Table 2 that D0₂₃ structure has the shorter Hf–Al bond length than D0₂₂ and L1₂ structures. It is known that a shorter bond length is related to a larger force constant and a higher vibrational frequency [31,32]. As a result, the phonon dispersions shift to the high frequency from L1₂, D0₂₂ to D0₂₃ structures in Fig. 4. The long-range Coulomb interactions result in the frequencies of longitudinal optical modes (LO) above those of transversal optical (TO) modes [33,34]. Due to insignificant LO/TO splitting in the high frequency, the influences of LO/TO splitting on the predicted thermodynamic properties are not considered in the present work.

Figure 5 plots the predicted thermodynamic properties of the L1₂, D0₂₂ and D0₂₃ HfAl₃ compounds. Their different thermodynamic properties curves with temperature confirm the fact of their different phonon dispersions. When the temperature increases, the enthalpy H and entropy S increase. The enthalpies of these HfAl₃ compounds increase almost linearly with temperature and tend to display $k_B T$ behavior, and this phenomenon can be observed in other Al-TM compounds [35]. The entropies of these compounds also increase rapidly with the increasing temperature when temperature is below 300 K, and the speed of increase

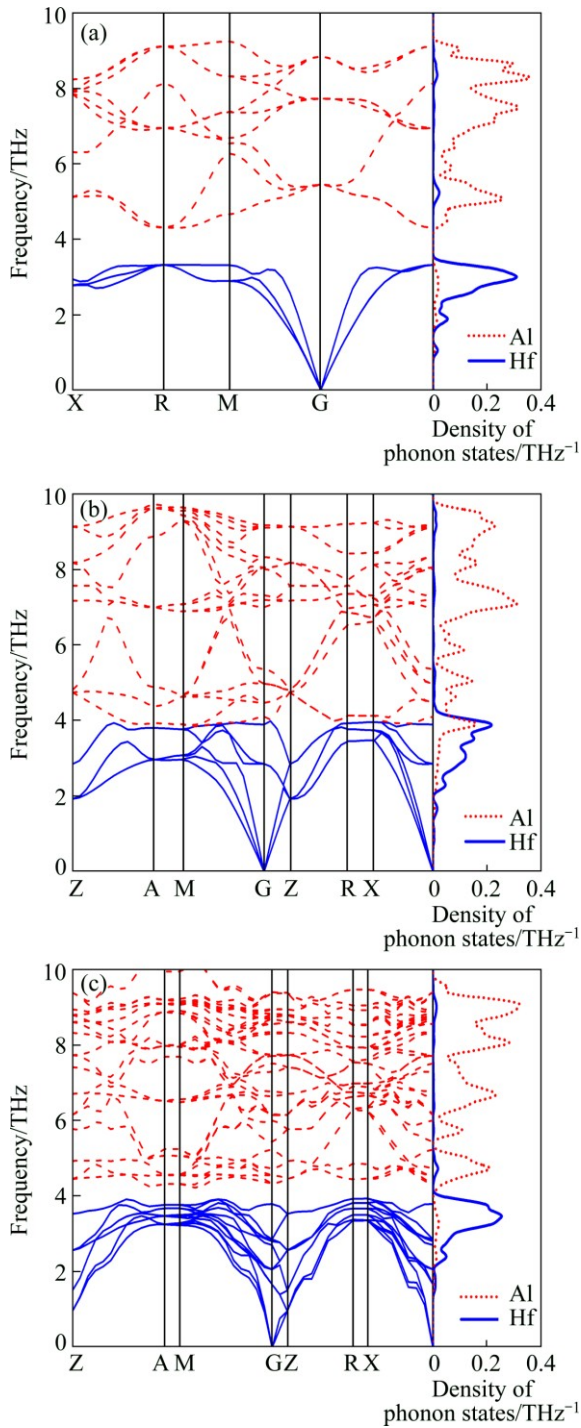


Fig. 4 Phonon dispersions and phonon density of states of HfAl_3 in L1_2 (a), D0_{22} (b) and D0_{23} (c) structures

slows down when temperature is above 300 K. Moreover, the H , S and F of D0_{23} structure change more quickly than those of the other two structures. It can be explained by the difference of phonon frequency. The free energy of D0_{23} structure is always lower than those of L1_2 and D0_{22} structures with the increase of temperature. In other words, in the range of temperature the order of free energy is $\text{D0}_{23} < \text{D0}_{22} < \text{L1}_2$, suggesting that the D0_{23} structure is always more stable than D0_{22}

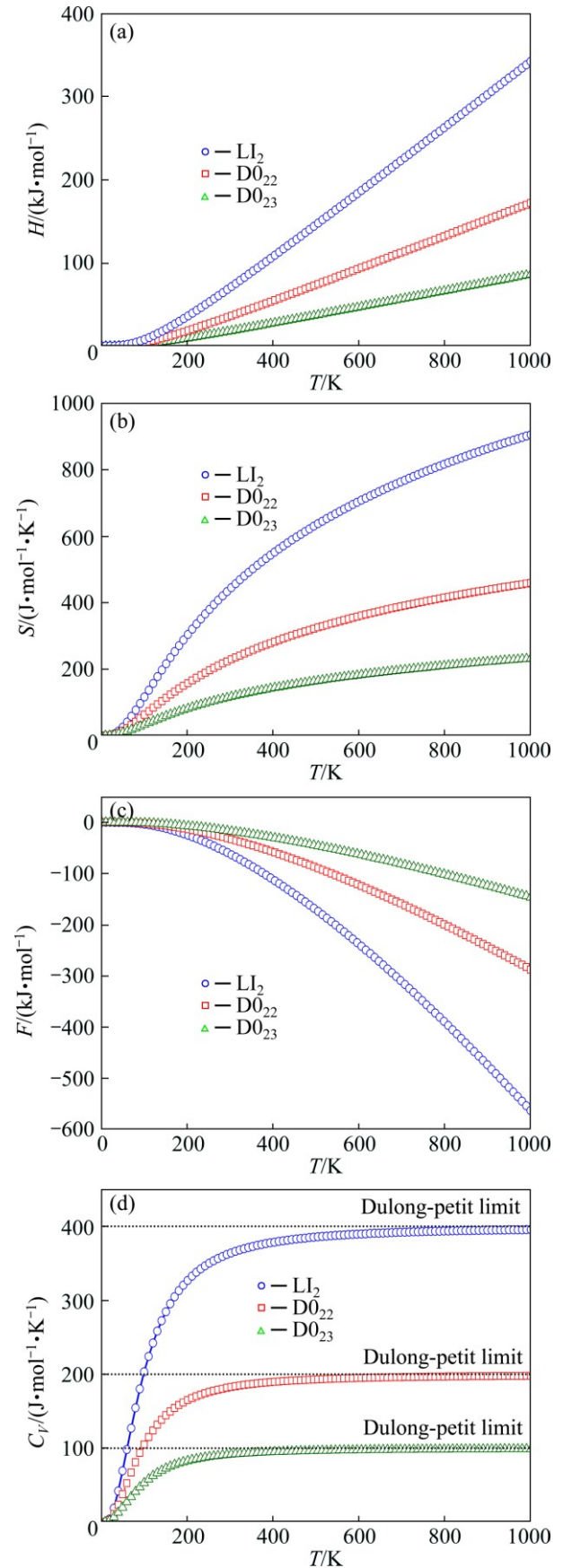


Fig. 5 Thermodynamic properties: enthalpy H (a), entropy S (b), free energy F (c) and specific heat capacity C_V (d) for HfAl_3 in L1_2 , D0_{22} and D0_{23} structures

and $L1_2$, and $L1_2$ structure is the most unstable phase. For the specific heat capacity C_V , it increases proportionally to T^3 at low temperature, and then gently at high temperature. When the temperature is higher than the Debye temperature, the specific heat capacity approaches to the Dulong–Petit limit: the specific heat capacities for the $L1_2$, $D0_{22}$ and $D0_{23}$ structures reach 100, 200 and 400 J/(mol·K) due to 4, 8, 16 atoms in their unit cells, respectively. The specific heat capacity C_V in Fig. 5 shows that the C_V of $D0_{23}$ structure increases more quickly than that of the other structures. It is similar to the variations of enthalpy H and entropy S . The reason is that the number of Hf atoms in $D0_{23}$ structure is four and the contribution from Hf atoms to the low phonon frequency is different from $L1_2$ and $D0_{22}$ structures. This leads to the diversity of phonon frequency in the Brillouin zone for the $D0_{23}$ structure.

The Debye temperatures of $L1_2$, $D0_{22}$ and $D0_{23}$ structures obtained from C_V are 399, 407 and 416 K, respectively. The theoretical Debye temperatures of $HfAl_3$ in the $L1_2$, $D0_{22}$ and $D0_{23}$ structures by ab initio calculations are 331, 335 and 334 K, respectively [15] which are obtained from the expression as $\Theta_D = K(r_{WS}B/M)^{1/2}$, where M is the atomic mass of the compound, r_{WS} is the Wigner-Seitz radius, B is the bulk modulus and K is a constant. In the ab initio calculations, the same K as obtained for pure aluminum is used in the $HfAl_3$ compounds, which results in lower Debye temperatures than our results. However, our Debye temperatures are close to each other, which is similar to the reported literature [15]. Such similar values of Debye temperatures lead to negligible differences in formation enthalpies at $T=0$ K. The Debye temperature is the temperature of a crystal's highest normal mode of vibration [36]. The similar values of Debye temperatures also suggest that the differences in the free energies even at high temperature $T < \Theta_D$ are small, which can be observed in Fig. 5.

Although the difference in Debye temperatures is small, the correlation between the calculated Debye temperatures (Θ_D) and the formation enthalpies (ΔH) of the $HfAl_3$ compounds has also been investigated. Interestingly, for these $HfAl_3$ compounds the Debye temperature is larger if the compound has a more negative formation enthalpy. Generally, a more negative formation enthalpy derives from stronger bonding. It is to be expected that a larger Debye temperature is an indicator of a stronger interatomic bonding. In the considered $HfAl_3$ compounds, the $D0_{23}$ structure has the largest Debye temperature (416 K) than the other structures, and it implies that the $D0_{23}$ structure has the most negative formation enthalpy (−39.224 kJ/mol). The experimental data are not available for the Debye

temperatures of $HfAl_3$ compounds. However, our calculated results can provide support for future works on these $HfAl_3$ compounds.

Figure 6 shows the volume thermal expansion coefficients of $HfAl_3$ in $L1_2$, $D0_{22}$ and $D0_{23}$ structures. From Fig. 6 it can be seen that at much less than the Debye temperature, the thermal expansion coefficients increase exponentially. This behavior is determined by thermal energy of lattice vibrations [37]. For example, when the temperature is lower than 200 K, the thermal energy of the lattice vibrations is increased rapidly due to the phonon excitations. The anharmonic effect is greatly enhanced in this temperature range. As a result, the volume thermal expansion coefficients increase quickly with respect to temperature. When the temperature is above 300 K, as shown in Fig. 6, the volume thermal expansion coefficients increase linearly versus temperature. Additionally, it should also be noted that the calculations of the thermal expansion coefficient are performed for the perfect crystal. The anharmonic effect is importantly influenced by the various defects (vacancies and impurities) in the real crystal. The total thermal energy of the lattice vibrations for a defective crystal is higher than that of perfect crystal. Thus, the thermal expansion coefficient for a real crystal is larger than the calculated value for a perfect crystal. This means that the true volume thermal expansion coefficients of these $HfAl_3$ compounds may be slightly larger than our calculated values. Meanwhile, in the Debye–Grüneisen model, bulk modulus B and Grüneisen parameter γ are theoretical ground-state values at the temperature lower than the Debye temperature. The ground-state values for B and γ suggest that the calculated thermal expansion coefficients are more accurate at the low temperature. In fact, the thermal expansion coefficients calculated by Debye–Grüneisen model at $T < 300$ K are in good agreement with the experiment data [38].

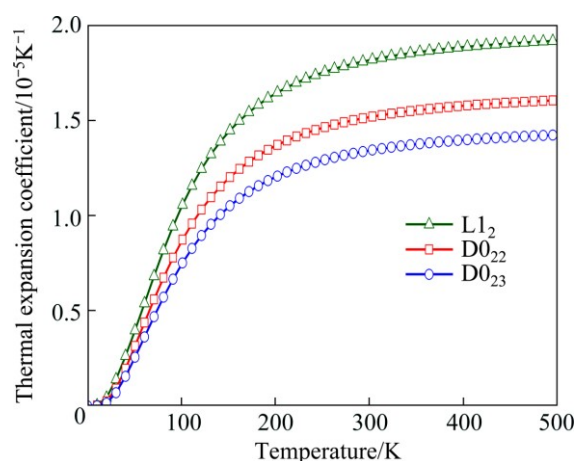


Fig. 6 Volume thermal expansion coefficients as function of temperature for $HfAl_3$ in $L1_2$, $D0_{22}$ and $D0_{23}$ structures

4 Conclusions

1) The calculated formation enthalpy shows that the structural stability of these three structures for HfAl_3 is in the order of $\text{D0}_{23} > \text{D0}_{22} > \text{L1}_2$.

2) The total densities of states for all structures have a similar shape characterized by the presence of pseudogap near the Fermi level (E_F). The E_F of D0_{23} structure is exactly located at the pseudogap, suggesting that the D0_{23} structure is the most stable.

3) No soft modes at any high-symmetry direction in the phonon dispersion curves are observed in the whole BZ, indicating that the current structures are thermodynamically stable.

4) The specific heat capacity C_V increases proportionally to T^3 at low temperature and approaches to the Dulong–Petit limit at the high temperature. The similar Debye temperatures of L1_2 , D0_{22} and D0_{23} structures obtained from C_V are 399, 407 and 416 K, respectively.

5) The volume thermal expansions for HfAl_3 increase exponentially at the low temperature, whereas the thermal expansion coefficients increase linearly at the high temperature.

References

- [1] SRINIVASAN S, DESCH P B, SCHWARZ R B. Metastable phase in the Al_3X (X=Ti, Zr, Hf) intermetallics system [J]. *Scripta Metallurgica et Materialia*, 1991, 25(11): 2513–2516.
- [2] VILLARS P, CALVERT L D. Pearson's handbook of crystallographic data for intermetallic phases [M]. Ohio: American Society for Metals, Materials Park, 1985.
- [3] MASSALSKI T B, OKAMOTO H, SUBRAMANIAN P R, KACPRZAK L. Binary alloy phase diagrams [M]. Ohio: ASM International, Materials Park, 1990.
- [4] HALLEM H, FORBORD B, MARTHINSEN K. An investigation of dilute Al–Hf and Al–Hf–Si alloys [J]. *Materials Science and Engineering A*, 2004, 387–389: 940–943.
- [5] MURRAY J L, MCALISTER A J, KAHAN D J. The Al–Hf (aluminum–hafnium) system [J]. *Journal of Phase Equilibria*, 1998, 19(4): 376–379.
- [6] PAXTON A T. Electron theory in alloy design [M]. London: The Institute of Materials, 1992.
- [7] VARIN R A, WINNICKA M B. Plasticity of structural intermetallic compounds [J]. *Materials Science and Engineering A*, 1991, 137: 93–103.
- [8] RYUM N. Precipitation in an Al–1.78 wt%Hf alloy after rapid solidification [J]. *Journal of Materials Science*, 1975, 10(12): 2075–2081.
- [9] HORI S, UNIGAME Y, FURUSHIR N, TAI H. Phase decomposition in splat quenched Al–6%Hf alloy [J]. *Journal of Japan Institute of Light Metals*, 1982, 32: 408–412.
- [10] FURUSHIRO N, HORI S. A possible mechanism of phase transformation of Al_3Hf from L1_2 to D0_{22} during aging in a rapidly solidified Al–3Hf–0.3Si alloy [J]. *Acta Metallurgica*, 1985, 33(5): 867–872.
- [11] PANDEY S K, SURYANARAYANA C. Structure and transformation behavior of a rapidly solidified Al–6.4 wt.%Hf alloy [J]. *Materials Science and Engineering A*, 1989, 111: 181–187.
- [12] NORMAN A F, TSAKIROPOULOS P. The microstructure and properties of rapidly solidified Al–Hf alloys [J]. *Materials Science and Engineering A*, 1991, 134: 1234–1237.
- [13] NORMAN A F, TSAKIROPOULOS P. Rapid solidification of Al–Hf alloys: Solidification microstructures and decomposition of solid solutions [J]. *International Journal of Rapid Solidification*, 1991, 6(3–4): 185–213.
- [14] SCHWARZ R B, DESCH P B, SRINIVASAN S, NASH P. Synthesis and properties of trialuminides with ultra-fine microstructures [J]. *Nanostructured Materials*, 1992, 1(1): 37–42.
- [15] COLINET C, PASTUREL A. Phase stability and electronic structure of the HfAl_3 compound [J]. *Physical Review B*, 2001, 64(20): 205102.
- [16] GHOSH G, ASTA M. First-principles calculation of structural energetics of Al-TM (TM= Ti, Zr, Hf) intermetallics [J]. *Acta Materialia*, 2005, 53(11): 3225–3252.
- [17] SEGALL M D, LINDAN P J D, PROBERT M J, PICKARD C J, HASNIP P J, CLARK S J, PAYNE M C. First-principles simulation: Ideas, illustrations and the CASTEP code [J]. *Journal of Physics: Condensed Matter*, 2002, 14(11): 2717–2744.
- [18] PERDEW J P, BURKE K, ERNZERHOF M. Generalized gradient approximation made simple [J]. *Physical Review Letters*, 1996, 77(18): 3865–3868.
- [19] FENG Jing, CHEN Jing-chao, XIAO Bing, DU Ye-ping, WANG Sheng-hao, ZHANG Li-juan. Oxidation and thermodynamic properties of Ag–Sn alloy [J]. *Acta Physico-Chimica Sinica*, 2008, 24(11): 2007–2012. (in Chinese)
- [20] BARONI S, de GIRONCOLI S, dal CORSO A, GIANNOZZI P. Phonons and related crystal properties from density-functional perturbation theory [J]. *Reviews of Modern Physics*, 2001, 73(2): 515.
- [21] DUAN Yong-hua, SUN Yong, FENG Jing, PENG Ming-jun. Thermal stability and elastic properties of intermetallics Mg_2Pb [J]. *Physica B: Condensed Matter*, 2010, 405(2): 701–704.
- [22] BLANCO M A, FRANCISCO E, LUANA V. GIBBS: isothermal-isobaric thermodynamics of solids from energy curves using a quasi-harmonic Debye model [J]. *Computer Physics Communications*, 2004, 158(1): 57–72.
- [23] HONG Q Z, LILIEFELD D A, MAYER J W. Thermal and ion-induced, metastable-cubic Al_3M phases in Al–Ti and Al–Hf thin films [J]. *Journal of Applied Physics*, 1988, 64(9): 4478–4483.
- [24] BOLLER H, NOWOTNY H, WITTMANN A. The crystal structure of hafnium-containing phases [J]. *Monthly Bulletin of Chemistry and Related Parts of Other Sciences*, 1960, 91(6): 1174–1184. (in German)
- [25] MAAS J, BASTIN G, VAN LOO F, METSELAAR R. On the texture in diffusion-grown layers of silicides and germanides with the FeB structure, MeX (Me= Ti, Zr; X= Si, Ge) or the ZrSi_2 structure [J]. *Z Metallkd*, 1983, 74: 294–299.
- [26] MESCHEL S V, KLEPPA O J. Standard enthalpies of formation of 5d aluminides by high-temperature direct synthesis calorimetry [J]. *Journal of Alloys and Compounds*, 1993, 197(1): 75–81.
- [27] WANG Tao, JIN Zhan-peng, ZHAO Ji-cheng. Thermodynamic assessment of the Al–Hf binary system [J]. *Journal of Phase Equilibria*, 2002, 23(5): 416–423.
- [28] CHENG Da-yong, ZHAO Shi-jin, WANG Sao-qing, YE Heng-qiang. First-principles study of the elastic properties and electronic structure of NiTi, CoTi and FeTi [J]. *Philosophical Magazine A*, 2001, 81(6): 1625–1632.
- [29] WANG Feng, SUN Shi-jie, YU Bo, ZHANG Feng, MAO Ping-li, LIU Zheng. First principles investigation of binary intermetallics in Mg–Al–Ca–Sn alloy: Stability, electronic structures, elastic

- properties and thermodynamic properties [J]. Transactions of Nonferrous Metals Society of China, 2016, 26(1): 203–212.
- [30] MAO Ping-li, YU Bo, LIU Zheng, WANG Feng, JU Yang. Mechanical and electronic structures of MgCu_2 , Mg_2Ca and MgZn_2 Laves phase by first principles calculations [J]. Transactions of Nonferrous Metals Society of China, 2014, 24: 2920–2929.
- [31] PENG Hua, WANG Chun-lei, LI Ji-chao, ZHANG Rui-zhi, WANG Mei-xiao, WANG Hong-chao, SUN Yi, SHENG Meng. Lattice dynamic properties of BaSi_2 and BaGe_2 from first principle calculations [J]. Physics Letters A, 2010, 374(36): 3797–3800.
- [32] LIU Yong, HU Wen-cheng, LI De-jiang, LI Ke, JIN Hua-lan, XU Ying-xuan, XU Chun-shui, ZENG Xiao-qin. Mechanical, electronic and thermodynamic properties of C14-type AMg_2 (A= Ca, Sr and Ba) compounds from first principles calculations [J]. Computational Materials Science, 2015, 97: 75–85.
- [33] PARLINSKI K. Lattice dynamics of cubic BN [J]. Journal of Alloys and Compounds, 2001, 328(1): 97–99.
- [34] ŁAŻEWSKI J, PARLINSKI K, SZUSZKIEWICZ W, HENNION B. Lattice dynamics of HgSe: Neutron scattering measurements and ab initio studies [J]. Physical Review B, 2003, 67(9): 094305.
- [35] DELIGOZ E, COLAKOGLU K, OZISIK H B, CIFTI Y O. Lattice vibrational properties of Al_2X (X= Sc, Y) from density functional theory calculations [J]. Solid State Communications, 2012, 152(2): 76–80.
- [36] LI Jian, ZHANG Ming, LUO Xian. Theoretical investigations on phase stability, elastic constants and electronic structures of D0_{22} - and L1_2 - Al_3Ti under high pressure [J]. Journal of Alloys and Compounds, 2013, 556: 214–220.
- [37] SUN Liang, GAO Yi-min, XIAO Bing, LI Ye-fei, WANG Guo-liang. Anisotropic elastic and thermal properties of titanium borides by first-principles calculations [J]. Journal of Alloys and Compounds, 2013, 579: 457–467.
- [38] MORUZZI V L, JANAK J F, SCHWARZ K. Calculated thermal properties of metals [J]. Physical Review B, 1988, 37(2): 790–799.

L1_2 、 D0_{22} 和 D0_{23} 结构 HfAl_3 的电子结构与热力学性质

李润岳¹, 段永华^{1,2}

1. 昆明理工大学 材料科学与工程学院, 昆明 650093;

2. 昆明理工大学 稀贵及有色金属先进材料教育部重点实验室, 昆明 650093

摘要: 为了更好地理解 L1_2 、 D0_{22} 和 D0_{23} 结构 HfAl_3 的相对稳定性和键合特征, 采用第一性原理计算了 L1_2 、 D0_{22} 和 D0_{23} 结构 HfAl_3 的形成焓、电子结构和热力学性质。结果表明: 平衡晶格参数与形成焓的计算结果与实验结果一致, 不同结构的 HfAl_3 稳定性大小为 $\text{D0}_{23} > \text{D0}_{22} > \text{L1}_2$; 态密度、电荷与键布局分析结果表明 D0_{23} 为最稳定结构; 声子计算得到的热力学性质与温度的关系表明, D0_{23} 结构的焓、熵和自由能随温度变化比 L1_2 和 D0_{22} 结构要快得多; L1_2 、 D0_{22} 和 D0_{23} 结构 HfAl_3 的德拜温度分别为 399、407 和 416 K; HfAl_3 的体积热膨胀系数在低温时成倍增加, 而在高温时线性增加。

关键词: 第一性原理; HfAl_3 ; 电子结构; 热力学性质

(Edited by Xiang-qun LI)